

# Source Parameters of Uttarkashi Earthquake of 21<sup>st</sup> Sept 2009

Arjun Kumar, Ashwani Kumar, Ashok Kumar, S.C. Gupta, A.K. Jindal and Himanshu Mittal

Department of Earthquake Engineering, Indian Institute of Technology, Roorkee, India.



## SUMMARY:

In the past four years, a permanent network of 35 strong motion accelerographs became operational in Garhwal Himalayas by Indian Institute of Technology, Roorkee (IITR). Another network of 12 short period stations is also being operated by IITR in Tehri region. These two networks recorded many earthquakes that occurred within this Garhwal Himalayan belt. One such earthquake is Uttarkashi earthquake of 21/9/2009 which occurred in vicinity of Uttarkashi earthquake of 20/10/1991 that took a toll of about 727 human lives, injured several thousand people and caused severe to partial damage to about 100,000 houses. This earthquake was widely recorded at 24 stations, 12 strong motion instruments and 12 short period instruments of Tehri network. This event occurred on 21<sup>st</sup> Sept 2009 at 09:43:52.3 (GMT) at latitude 30.837N, longitude 78.984E, depth 53.3 km have magnitude of 4.7. Only a few events were occurred at a depth greater than 45 km in this region. This event occurred at the foot of main central thrust (MCT) and has (strike: 263.42, dip: 66.84, rake: 36.07) strike-slip trend with normal faulting component, however the Uttarkashi earthquake of 1991 has thrust faulting. In this study Brune's model that yield a fall-off of 2 beyond corner frequency is considered with high frequency diminution factor, a Butterworth high-cut filter presented by Boore (1983) that fits well for frequencies greater than  $f_{max}$ . The seismic moment for this event has been found to be of the order of  $(107 \pm 0.19) \times 10^{23}$  dyne.cm and the moment magnitude has been calculated  $4.7 \pm 0.09$  at different stations. The stress drop is found to be  $76.3 \pm 11.5$  bars, while source radius for the earthquake is estimated to be  $(850.0 \pm 38.0)$  m. The value of  $f_{max}$  for this earthquake is  $9.1 \pm 1.7$  Hz obtained from records at various stations of different site conditions. However, this single event data is not sufficient to conclude whether  $f_{max}$  is a source or site related phenomenon.

*Key words: IITR, Garhwal, Uttarkashi, MCT, 21<sup>st</sup> Sept 2009*

## 1. INTRODUCTION

The shape of the seismic spectrum and how it scales with earthquake size has been a topic of importance as a way of gaining insight into the character of earthquake source processes and also as a guide to the simulation of strong ground motion for engineering purposes (Joyner, 1984).

Aki (1967) made first effort in this direction by examining the dependence of the amplitude spectrum of seismic waves on source size on the basis of two dislocation models of an earthquake source. One of the models (by N. Haskell) is called the  $\omega^3$  model, and the other, called the  $\omega^2$  model, is constructed by fitting an exponentially decaying function to the autocorrelation function of the dislocation velocity. The  $\omega^2$  model gives a satisfactory agreement with such observations on the assumption of similarity, but the  $\omega^3$  model does not. He made these models considering a constant stress drop. However, he pointed out that if the stress drop differs, the scaling law will not apply. If the stress drop varies systematically with respect to environmental factors as focal depth, orientation of the fault plane, crust-mantle structure, we may construct different scaling laws for different environments.

Brune (1970, 1971) modeled an earthquake source as a tangential stress pulse applied instantaneously to the interior of a dislocation surface. This model employs three independent parameters (moment, source dimension and fractional stress drop) those determine the shape of the far-field displacement spectrum of

body waves. He constrained the relationship of the corner frequency of the fault radius by assuming that the effective stress was equal to the average static stress drop.

Since then a number of studies have been carried out over the world and showed that for small to large earthquakes the stress drop is mainly independent of the size in terms of moment of earthquake (e.g., Kanamori and Anderson, 1975; Fletcher, 1980; Archuleta et al., 1982; Hanks and Boore 1984; O'Neill, 1984; Andrews, 1986; Sharma and Wason, 1994; Amberg, 1995; Bansal, 1998). The constant-stress-drop model also implies a self-similar rupture process that is independent of the size of the earthquake and that seismic moment is proportional to the cube of the source radius, after Brune (1970, 1971). On the other side many studies that suggest a breakdown in self-similarity between large and small events at a seismic moment of roughly  $10^{13}$  N-m (Fletcher et al. 1986, Gibowicz and Kijko, 1994). This apparent breakdown in self similarity is closely linked to causes that limit high-frequencies,  $f_{max}$  (Hanks, 1982) of the radiated wave field (Jost et al. 1998).

In the present study source parameters, namely: seismic moment, source dimension and stress drop have been computed using 24 station data for earthquake that occurred on 21<sup>st</sup> September 2009 north of MCT and close to the Uttarkashi earthquake of 1991. SH-components of all stations have been analyzed employing Brune's model.

## 2. SEISMOTECTONICS OF THE STUDY AREA

The convergence between India and Tibet has continued for more than 50 million years after their initial contact in Cretaceous times and has resulted in the development of two northerly deeping interpolate convergent zones viz. the main Central Thrust (MCT) and the main Boundary Thrust (MBT) (e.g. Valdiya, 1981). The MBT separates Lesser Himalaya from the Sub-Himalaya belt while the MCT separates the Higher Himalaya from the Lesser Himalaya. A majority of the earthquakes of the Indian region occur in the Himalaya as a result of collision between India and Tibet (Gansser, 1964; Valdiya, 1981; Ni and Barazangi, 1984; Molnar, 1990).

One of the earliest earthquakes reported in this area by IMD is of magnitude 6.5 which occurred on July 15, 1720 at Latitude  $28.37^{\circ}$  N and Longitude  $77.1^{\circ}$  E. The prominent earthquakes experienced by this region are (i) Feb 28, 1906 with magnitude 7.0, (ii) June 04, 1945 with magnitude 6.5, (iii) Feb 23, 1953 with magnitude 6.0, (iv) July 14, 1962 with magnitude 5.5, (v) July 29, 1980 Dharchula earthquake with magnitude 6.1 (vi) Uttarkashi earthquake of Oct 20, 1991 of magnitude 6.4 and (vii) Chamolli earthquake of March 29, 1999 of magnitude 6.8.

The seismotectonic map of the study area along with the locations of the Uttarkashi earthquake of 20<sup>th</sup> October 1991 and the location of the 21<sup>st</sup> Sept 2009 event considered in the present study as well as instrument locations are shown in Figure 1.

## 3. DATA SOURCE

The data collected by Indian Institute of Technology, Roorkee (IITR) during different earthquakes is used for estimation of source parameters. IITR installed 300 strong motion accelerographs in North and NE India covering seismic zones V, IV and some thickly populated cities of seismic zone III under a project sponsored by Ministry of Earth Sciences, Government of India. This network used GSR-18 (Geosig , model GSR-18 sampling rate 200 Hz) digital instruments and used best possible communication facilities to network these instruments. The instruments have installed in the states of HP, Punjab, Haryana, Rajasthan, Uttarakhand, UP, Bihar, Sikkim, West Bengal, A&N, Meghalaya, Mizoram and Assam. Out of 300, 37 instruments are installed in Uttarakhand to closely monitor the seismic activity in Himalayas

(Kumar et. al., 2012). Fig. 1 shows the location of instruments by solid magenta triangles in Uttarakhand. This network recorded this earthquake at 12 stations.

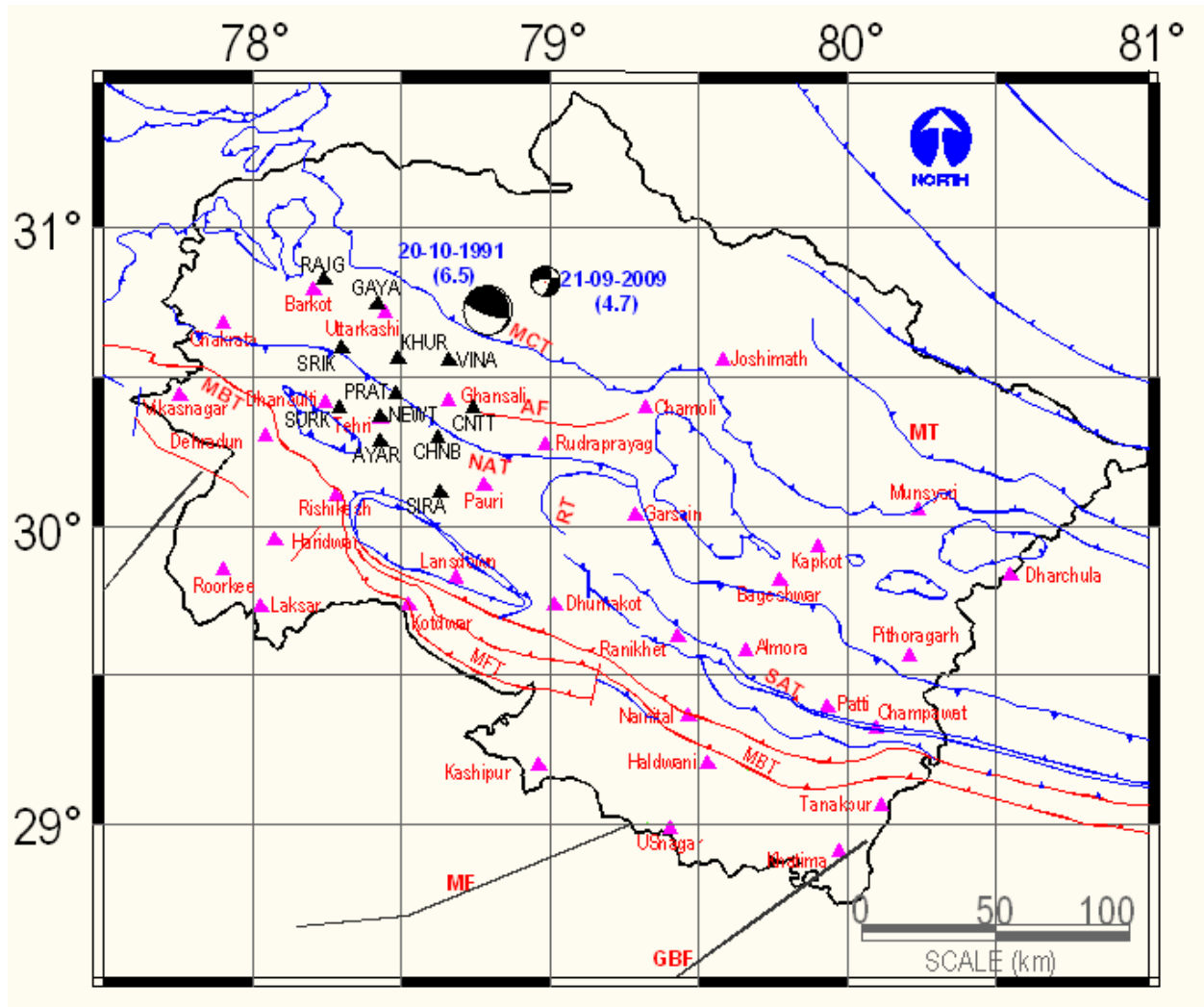


**Figure 1:** Seismotectonic map of Uttarakhand (tectonics after GSI, 2000) along with the location of instruments, strong motion (magenta triangles) and short period (black triangles). The location of 20/10/1991 and 21/09/2009 earthquakes used in present study are shown by their respective fault plane solutions.

IIT Roorkee also installed 12-station (Guralp, triaxial short-period seismometer model CMG 40T-1, sampling rate 100 Hz) local seismological network in and around Tehri region under a project sponsored by Tehri Hydro Development Corporation India Ltd. (THDCIL). This network has been deployed for the purpose of collecting data of local earthquakes around Tehri region to study the attributes of the local seismicity in the environs of 260.5 m high Tehri dam. The network is shown in Figure 1 by solid black triangles. This network recorded the earthquake at all 12 stations.

#### 4. METHODOLOGY

The time histories are first rotated to obtained SH-component of ground motion and then spectrum is corrected for instrument response and attenuation due to path. In this study Brune's model that yield a fall-off of 2 beyond corner frequency is considered with high frequency diminition factor, a Butterworth

high-cut filter presented by Boore (1986) that fits well for frequencies greater than  $f_{max}$  is fitted in observed acceleration spectrum as

$$A(R, f) = \frac{(2\pi f)^2 \Omega_0}{1 + \left(\frac{f}{f_c}\right)^2} \left[1 + \left(\frac{f}{f_{max}}\right)^N\right]^{-1/2}$$

And for displacement spectrum

$$D(R, f) = \frac{\Omega_0}{1 + \left(\frac{f}{f_c}\right)^2} \left[1 + \left(\frac{f}{f_{max}}\right)^N\right]^{-1/2}$$

Computer software is developed that automatically picks the spectral parameters:

1. low frequency displacement spectral level,  $\Omega_0$ ,
2. corner frequency above which spectrum decays with a rate of 2,  $f_c$ ,
3. the frequency above which the spectrum again decays,  $f_{max}$  and
4. the rate of decay above  $f_{max}$ ,  $N$ .

The seismic moment is estimated from the value of  $\Omega_0$  as

$$M_o = \frac{4\pi\rho\beta^3 R\Omega_0}{R_{\theta\phi} S_a} \quad [\text{Kellis-Borok, 1960}]$$

Here  $\rho$  is the average density ( $=2.67 \text{ g/cm}^3$ ),  $\beta$  is shear wave velocity in the source zone ( $=3.2 \text{ km/s}$ ),  $R$  is the hypocentral distance,  $R_{\theta\phi}$  is the average radiation pattern ( $=0.63$ ),  $S_a$  is free surface amplification ( $=2$ ).

The moment magnitude,  $M_\omega = \frac{2}{3} \log(M_o) + 10.7$  [Hanks and Kanamori, 1979]

The source radius,  $r = \frac{2.34\beta}{f_c}$  [Brune, 1970, 1971]

The stress drop,  $\Delta\sigma = \frac{7M_o}{16r^3}$  [Brune, 1970, 1971]

## 5. RESULTS AND DISCUSSION

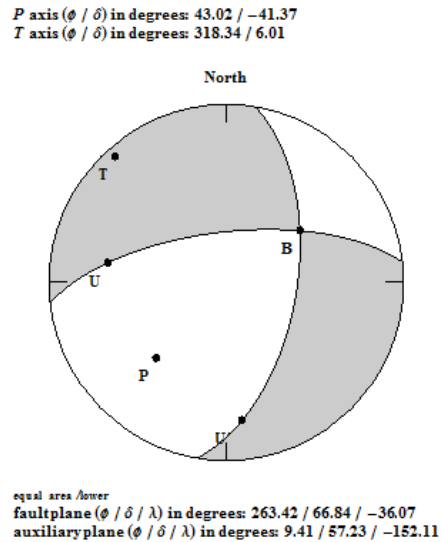
The P-wave and S-wave arrival time data (phase-data) from the 12 digital seismograms and 12 strong motion records have been used to compute the hypocenter parameters. The HYPOCENTER (Lienert et al., 1986) computer program has been employed for this purpose and computations have been carried out adopting the earthquake analysis software SEISAN (Havskov and Ottemöller, 2005). The hypocenter parameters along with standard errors are listed in Table 1 and the location is shown in Figure 1.

Table 1. Hypocenters parameters of located earthquake.							
Origion Time ( GMT)	Latitude ° N	Longitude ° E	Depth (km)	M <sub>L</sub>	RMS (km)	ERH (km)	ERZ (km)
20090921 09:43:52.3	30.837	78.984	53.3	4.8	0.2	2.1	2.5

The first motion polarity data from 24 stations has been used to draw the fault plane solution using SEISAN (Havskov and Ottemöller, 2005) software that uses the program FOCMEC (Snoke et. al., 1984). The fault plane solution obtained is plotted by "Earthquake Focal Mechanism" from the Wolfram Demonstrations Project is given below:

**Table 2.** Fault plane solution of 21/09/2009 earthquake.

Strike	Dip	Rake
263.42	66.84	-36.07



The rotated time histories and the selected part of SH-component used for analysis from seismogram (Vinakhal) and strong motion instrument (Dhanolti) are shown in Figures 2 and Figure 3. The acceleration and displacement spectra along with the fitted model are also shown below in respective figures.

21/09/2009 VINA

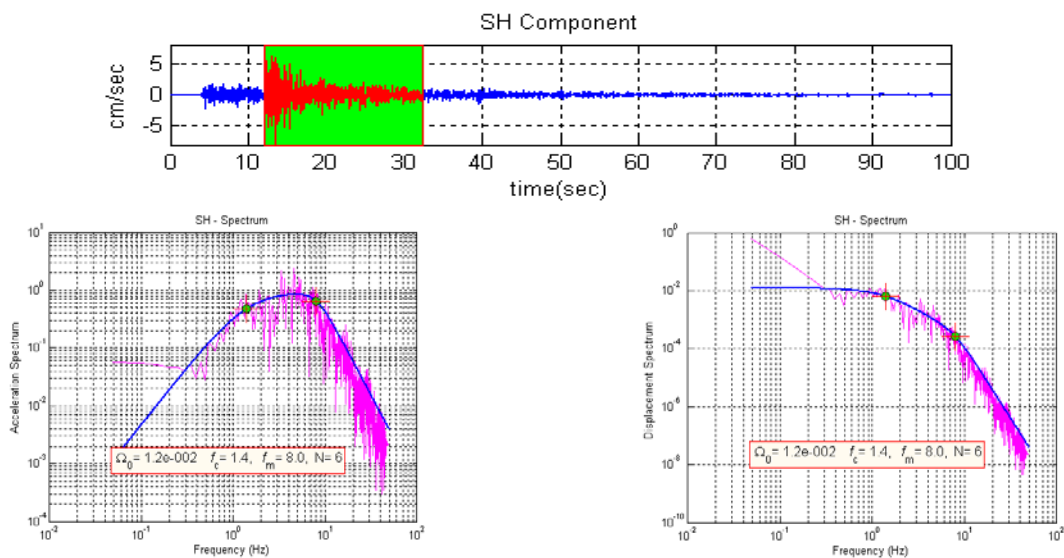


**Figure 2** An example of SH component of velocity time history of earthquake recorded at Vinakhal on short period seismograph. The acceleration and displacement spectra along with fitted source model.

21/09/2009 DHANOLTI

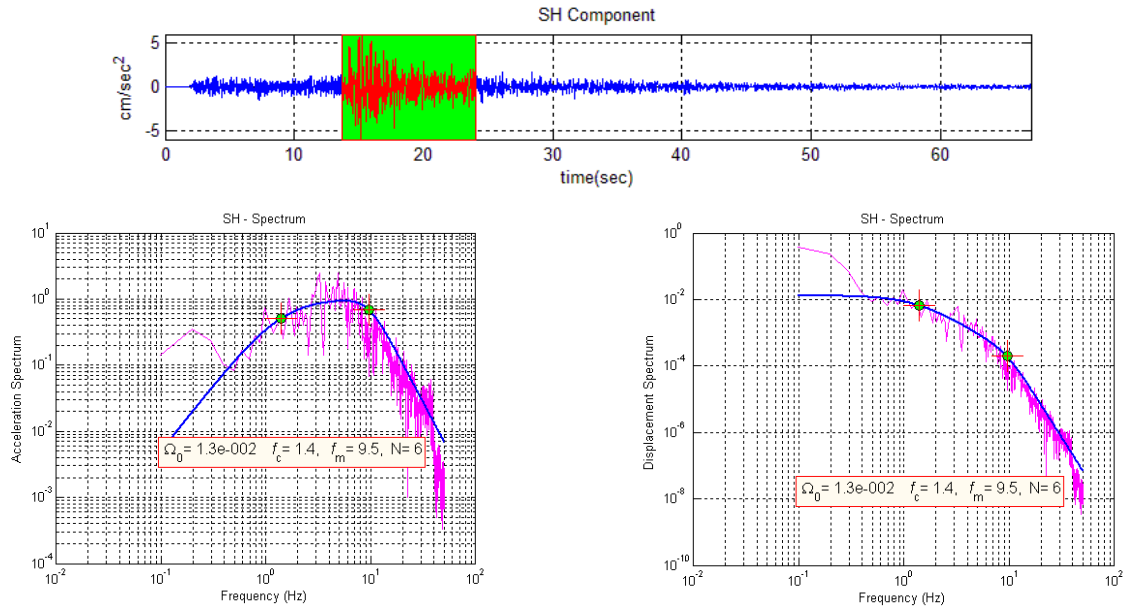


**Figure 3.** An example of SH component of acceleration time history of earthquake recorded at Dhanolti on strong motion instrument. The acceleration and displacement spectra along with fitted source model.

The spectral parameters obtained from the velocity and acceleration records at various sites are given below along with estimated source parameters in Table 3.

**Table 3.** Spectral parameters and the estimated source parameters of 21/09/2009 earthquake.

Station	$f_c$	$f_{max}$	$N$	$\Omega_0$ cm	$M_0$ (dyne cm)	$M\omega$	$R$ (m)	$\Delta\sigma$ (bars)
AYAR	1.4	12	6	0.013	1.30381E+23	4.7	850.9	92.586
CHNB	1.4	8.5	6	0.013	1.22807E+23	4.7	850.9	87.207
CNTT	1.4	9	4	0.011	9.59596E+22	4.7	850.9	68.142
GAYA	1.3	9	6	0.014	1.27248E+23	4.7	916.4	72.348
KHUR	1.4	9	8	0.013	1.17178E+23	4.7	850.9	83.210
NEWT	1.4	8	6	0.011	1.07837E+23	4.7	850.9	76.577
PRAT	1.4	6.5	6	0.01	9.39507E+22	4.6	850.9	66.716
RAJG	1.3	8	8	0.011	1.0914E+23	4.7	916.4	62.053
SIRA	1.4	10	8	0.012	1.21389E+23	4.7	850.9	86.199
SRIK	1.3	8	6	0.014	1.37265E+23	4.8	916.4	78.043
SURK	1.3	7	6	0.014	1.43406E+23	4.8	916.4	81.535
VINA	1.4	8	6	0.012	1.01265E+23	4.7	850.9	71.909
Bageshwar	1.5	12	6	0.0063	7.75071E+22	4.6	794.2	67.695
Barkot	1.4	8.5	6	0.011	1.1087E+23	4.7	850.9	78.730
BHAWANGR	1.4	7	6	0.0062	9.96284E+22	4.7	850.9	70.747
Chamoli	1.4	7	6	0.01	8.96287E+22	4.6	850.9	63.647
Dhanaulti	1.4	9.5	6	0.013	1.35079E+23	4.8	850.9	95.921
Garsain	1.5	10	6	0.011	1.14103E+23	4.7	794.2	99.658

Ghansali	1.4	9	6	0.013	1.15201E+23	4.7	850.9	81.806
Jubbal	1.5	12	6	0.0069	8.69694E+22	4.6	794.2	75.959
Kapkot	1.4	12.5	6	0.0078	9.60894E+22	4.7	850.9	68.234
Lansdown	1.5	8	6	0.006	6.77254E+22	4.6	794.2	59.152
Rampur	1.4	9	6	0.006	7.89837E+22	4.6	850.9	56.087
Rudraprayag	1.5	10	6	0.011	9.90123E+22	4.7	794.2	86.478

The seismic moment for this event has been found to be of the order of  $(1.07 \pm 0.19) \times 10^{23}$  dyne.cm and the moment magnitude has been calculated  $4.7 \pm 0.09$  at different stations. The stress drop is found to be  $76.3 \pm 11.5$  bars, while source radius for the earthquake is estimated to be  $(850.0 \pm 38.0)$  m. The value of  $f_{max}$  for this earthquake is  $9.1 \pm 1.7$  Hz obtained from records at various stations of different site conditions. A change in spectral fall-off above  $f_{max}$  has been observed in short period instruments while strong motion instruments has same value. This may be due to different band-width of recording instruments.

In the earthquake source models the acceleration spectrum increases with increasing frequency and become constant beyond corner frequency. Hanks (1982) observed that there is another frequency called the maximum cut-off frequency  $f_{max}$ , above which acceleration spectral amplitudes diminish abruptly. There is a controversy about the origin of this cut-off frequency  $f_{max}$ . Hanks (1982) and Anderson and Hough (1984), among others, contend that  $f_{max}$  is a recording site effect while Papageorgiou and Aki (1983a, b) and Yokai and Irikura (1991) attribute it to a source effect. Tsai and Chen (2000) fitted a regression model in terms of distance, earthquake magnitude, and site and showed that the high-cut process is controlled by both the site and source effects. They also inferred that distance is the least significant parameter controlling the high-cut process.

However this single event data from 24 stations is not sufficient to conclude whether  $f_{max}$  is a source or site related phenomenon.

## CONCLUSION

The estimated stress drop for this event is  $76.3 \pm 11.5$  bars that is higher than the stress drop of  $52.6 \pm 5.9$  bars for Uttarkashi earthquake of 1991 and an average of about 60 bars for Garhwal-Kumaon Himalayan earthquakes (Kumar, 2011). This event occurred at a depth of 53.3 km in the foot of MCT and has (strike: 263.42, dip: 66.84, rake: 36.07) strike-slip trend with normal faulting component, however the Uttarkashi earthquake of 1991 occurred at a depth 12 km and has thrust faulting. The difference in focal depth and the trend of faulting may be the cause of higher stress drop in this earthquake.

## ACKNOWLEDGMENT

The authors are profusely thankful to Ministry of Earth Sciences (MoES) and Tehri Hydro Power Development Corporation (THDC) for funding all projects under which data was collected.

## REFERENCES

- Aki, K. (1967). Scaling law of seismic spectrum, *J. Geophys. Res.* **72**, 1217-1231.  
 Abercrombie, R.E. (1995). Earthquake source scaling relationships from -1 to 5  $M_L$  using seismograms recorded at 2.5 km depth, *J. Geophys. Res.* **100**, 24015-24036.  
 Anderson, J.G. and Hough, S.E. (1984). A model for the shape of the Fourier amplitude spectrum of acceleration at high frequencies, *Bull. Seism. Soc. Am.* **74**, 1969-1993.  
 Archuleta, R.J., Cranswick, E., Mueller, C. and Spudis, P. (1982). Source parameters of the 1980 Mammoth lakes, California, earthquake sequence. *J. Geophys. Res.* **87**, 4595- 4607.

- Bansal, B. K. (1998). Determination of source parameters for small earthquake in the Koyna region, *11<sup>th</sup> Symposium on Earthquake Engineering, Roorkee* Vol. 1, 57- 66.
- Boore, D. M. (1986). Short-period P- and S-wave radiation from large earthquakes: Implications for spectral scaling relations, *Bull. Seism. Soc. Am.* **76**, 43-64.
- Brune, J. N. (1970). Tectonic stress and the spectra of seismic shear waves from earthquakes: *J. Geophys. Res.* **75**, 4997-5009.
- Brune, J. N. (1971). Correction to tectonic stress and the spectra of seismic shear waves from earthquakes, *J. Geophys. Res.* **76**, 5002.
- Fletcher, J.B. (1980). Spectra from high dynamic range digital recordings of Oroville, California, aftershocks and their parameters, *Bull. Seismol. Soc. Am.* **70**, 735-755.
- Scherbaum, F., N. Kuehn, and B. Zimmermann. "Earthquake Focal Mechanism" from the Wolfram Demonstrations Project. <http://demonstrations.wolfram.com/EarthquakeFocalMechanism/>
- Ganser, A. (1964). *Geology of the Himalayas*, London: Wiley Interscience.
- Gibowicz, S.J. and Kijko, A. (1994). *An Introduction to Mining Seismology*. Academic Press.
- GSI (2000). Seismotectonic Atlas of India and its Environs. *Geol. Surv. India*, Sp. Pub., P. L. Narula, S. K. Acharya and J. Banerjee (eds.).
- Hanks, T.C. (1982).  $f_{max}$ , *Bull. Seism. Soc. Am.* **72**, 1869-1879.
- Hanks, T.C., and Boore, D.M. (1984). Moment-Magnitude relations in theory and practice, *J. Geophys. Res.* **89**, 6229-6235.
- Hanks, T.C., and Kanamori, H. (1979). A moment magnitude scale: *J. Geophys. Res.* **84**, 2348-2350.
- Havskov Jens and Ottemoller Lars (2005). *Seisan: The Earthquake Analysis Software*. Version 8.1.
- Jost, M.L., Büfelberg, T. Jost, Ö and Harjes, H.-P. (1998). Source parameters of injection-induced microearthquakes at 9 km depth at the KTB Deep Drilling site, Germany. *Bull. Seism. Soc. Am.* **88**, 815-832.
- Kumar, A. (2011). Study of earthquake source parameters using microearthquakes and strong motion data, *Thesis submitted to Indian Institute of Technology, Roorkee*.
- Kumar, A., Mittal, H., Sachdeva, R. and Kumar, A. (2012). Indian National Strong Motion Network, *Seism. Res. Lett.* **83:1**, 29-36.
- Joyner, W. S. (1984). A scaling law for the spectra of large earthquakes, *Bull. Seism. Soc. Am.* **74:4**, 1167-1188.
- Kanamori, H. and D. L. Anderson (1975). Theoretical basis of some empirical relations in seismology, *Bull. Seism. Soc. Am.* **65**, 1073-1095.
- Keilis-Borok, V. I. (1960). Investigation of the mechanism of earthquakes: *Sov. Res. Geophys., (English transl.)* **4**, 29.
- Lienert, B.R., Berg, E. and Frazer, L.N. (1986). Hypocenter: An earthquake location method using centered, scaled, and adaptively least squares. *Bull. Seismol. Soc. Am.* **76**, 771-783.
- Molnar, P. (1990). A review of the seismicity and the rates of active underthrusting and deformation at the Himalaya, *J. Him. Geol.* **1**, 131-154.
- Ni, J. and Barazangi, M. (1984). Seismotectonics of the Himalayan Collision Geometry of the Underthrusting Indian Plate Beneath the Himalaya, *J. Geophys. Res.* **89**, 1147- 1163.
- O'Neill, M.E. (1984). Source dimensions and stress drops of small earthquakes near Parkfield, California, *Bull. Seism. Soc. Am.* **71**, 27-40.
- Papageorgiou, A.S. and Aki, K. (1983a). A specific barrier model for the quantitative description of inhomogeneous faulting and the prediction of strong ground motion. I. Description of the model, *Bull. Seism. Soc. Am.* **73**, 693-722.
- Papageorgiou, A.S. and Aki, K. (1983b). A specific barrier model for the quantitative description of inhomogeneous faulting and the prediction of strong ground motion. II. Application of the model, *Bull. Seism. Soc. Am.* **73**, 953-978.
- Sharma, M.L. and Wason, H.R. (1994). Occurrence of low stress drop earthquakes in the Garwal Himalayan region. *Physics of the Earth and Planetary Interiors* **85**, 265-272.
- Snoke, J.A., Munsey, J.W., Teague, A.G., and Bollinger, G.A. (1984). A program for focal mechanism determination by combined use of polarity and SV-P amplitude ratio data. *Earthquake notes*, **55**.
- Tsai, C.-C. P. and Chen, K.C. (2000). A model for the high-cut process of strong-motion accelerations in terms of distance, magnitude, and site condition: An example from the SMART 1 array, Lotung, Taiwan, *Bull. Seism. Soc. Am.* **90:6**, 1535-1542.
- Valdiya, K.S. (1981). The tectonics of the central sector of the Himalaya. In: H.K. Gupta and F.M. Delany (Eds.), *Zagros-Hindukush-Himalaya: Geodynamic Evolution, Amer. Geophys. Union, Washington*, 87-110.
- Yokoi, Toshiaki and Kojiro Irikura (1991). Meaning of source controlled  $f_{max}$  in empirical Green's function technique based on a  $T^2$ -scaling law, *Annuals, Disas. Prev. Res. Inst., Kyoto Univ.* **34 B- 1**.